A Morphodynamic Link Between Grain Size and Delta Morphology

Rebecca L. Caldwell[1*], Douglas A. Edmonds[1]

[1]Department of Geological Sciences, Indiana University

1001 East 10th Street, Bloomington, IN, 47405, *relecald@indiana.edu

I. ABSTRACT

Delta morphology is traditionally explained by differences in fluvial energy and wave and tidal energy. However, deltas influenced by similar ratios of river to marine energy can display strikingly different morphologies. Other variable, such as grain size of the sediment load delivered to the delta, influence delta morphology, but these models are largely qualitative, leaving many questions unanswered. To better understand how grain size modifies deltaic processes and morphologies we conducted 33 numerical modeling experiments using the morphodynamic physics-based model Delft3D and quantified the effects produced by different grain sizes. In these 33 runs we change the median (0.01 – 1 mm), standard deviation (0.1 – 3 φ), and skewness(-0.7 – 0.7) of the incoming grain-size distribution. The model setup includes a river carrying constant discharge entering a standing body of water devoid of tides, waves, and sea-level change. The results show that delta morphology undergoes a transition as median grain size and standard deviation increase while changing skewness has little effect. At low median grain size and standard deviation, deltas have elongate planform morphologies with sinuous shorelines characterized by shallow topset gradients ranging from 1×10^{-4} to 3×10^{-4}, and 1 – 8 stable active channels. At high median grain size and standard deviation, deltas transition to semi-circular planform morphologies with smooth shorelines characterized by steeper topset gradients ranging from 1×10^{-3} to 2×10^{-3}, and 14 – 16 mobile channels. The change in delta morphology can be morphodynamically linked to changes in grain size. As grain size increases delta morphology transitions from elongate to semi-circular because the average topset gradient increases. For a given set of flow conditions, larger grain sizes require a steeper topset gradient to mobilize and transport. The average topset gradient reaches a dynamic equilibrium through time. This requires that, per unit length of seaward progradation, deltas with steeper gradients have higher vertical sedimentation rates. Higher sedimentation rates, in turn, perch the channel above the surrounding floodplain (so-called 'super-elevation') resulting in unstable channels that frequently avulse and create periods of overbank flow. That overbank flow is more erosive because the steeper gradient causes higher shear stresses on the floodplain, which creates more channels. More channels reduce the average water and sediment discharge at a given channel mouth, which creates time scales for mouth bar formation in coarse-grained deltas that are longer than the avulsion time scale. This effectively suppresses the process of bifurcation around river mouth bars in coarse-grained deltas, which in turn creates semi-circular morphologies with smooth shorelines as channels avulse across the topset. On the other hand, finest-grained (i.e. mud) deltas have low topset gradients and fewer channels. The high water and sediment discharge per channel, coupled with the slow settling velocity of mud, advects the sediment far from channel mouths, which in turn creates mouth bar growth and avulsion time scales that are longer than the delta life. This creates an elongate delta as stable channels prograde basinward. Deltas with intermediate grain sizes have nearly equal avulsion and bifurcation time scales, creating roughly semi-circular shapes but with significant shoreline roughness where mouth bars form.

II. STATEMENT OF THE PROBLEM

Delta morphology has traditionally been explained by differences in river, wave, or tidal energy, yet deltas influenced by similar ratios of marine to river energy can display strikingly different morphologies (Fig. 1). This suggests that delta morphology may be controlled by additional variables. Previous research has qualitatively noted that grain size can influence delta morphology (Fig. 2), but a clear mechanistic understanding of this is lacking.

Here we quantify grain size effects on delta morphology and present a process-based understanding of how grain size influences deltaic processes, and thus morphology.

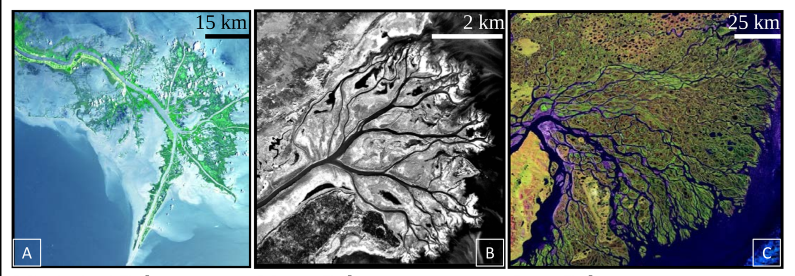

Figure 1. Deltas with similar ratios of marine to fluvial energy (M_p:R_p) have different morphologies from elongate (A) to semi-circular (B) to braided (C). Data from Syvitski and Saito (2007) and Edmonds (unpublished).

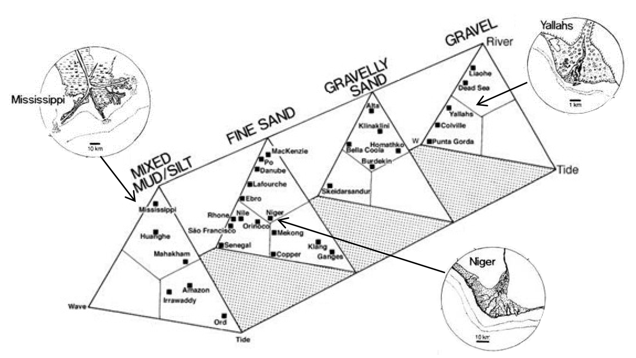

Figure 2. Delta morphology is related to grain size in addition to river, wave, and tidal energy. (from Orton and Reading, 1993).

III. METHODOLOGY

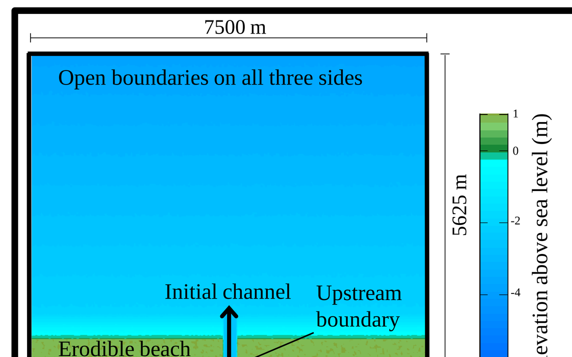

Figure 3. Numerical model setup. Each grid cell size is 25 x 25 m.

To meet our goals we numerically model delta growth, changing only the incoming grain-size distribution.

We use Delft3D, a morphodynamic physics-based model that calculates:

- Hydrodynamics → depth-integrated Reynolds-averaged Navier-Stokes equations
- Sediment transport → Van Rijn (1993), (suspended and bedload)
- Bed evolution → Exner equation

- The model setup consists of an initial channel (width = 250 m, depth = 2.5 m) entering a gently sloping basin, devoid of waves, tides, sea-level change, and buoyancy forces (Fig. 3).
- Upstream boundary conditions include constant water discharge of 1000 m^3/s, suspended sediment load of 0.1 kg/m^3, and equilibrium bed load flux.
- Downstream boundary conditions include uniform water surface elevations.
- We vary the incoming grain-size distribution in three ways: (1) median (D_{50}) [0.01 – 1 mm]; (2) standard deviation (σ) [0.1-3 φ]; (3) skewness (sk) [-0.7 – 0.7].

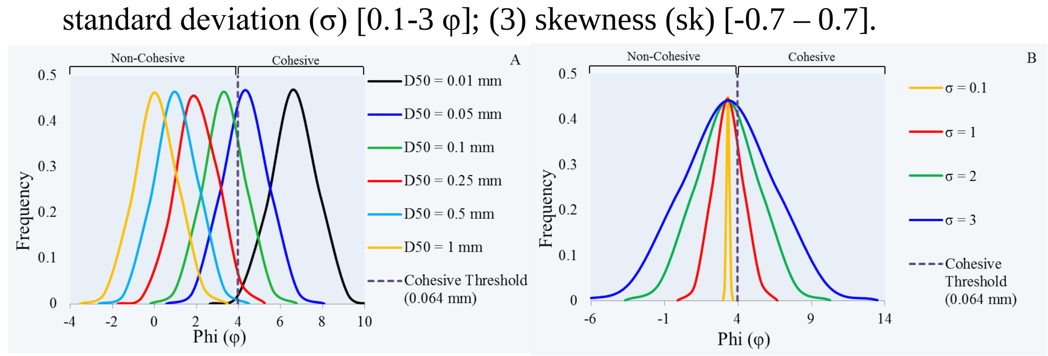

- For every D_{50} (Fig. 4A) we change σ over four increments (Fig. 4B) to produce a total of 23 runs with unique combinations of D_{50} and σ.

Figure 4. Example grain-size distributions for (A) different median grain sizes (σ =1 φ, sk=0), and (B) different standard deviations (D_{50}= 0.1 mm, sk= 0).

IV. Results

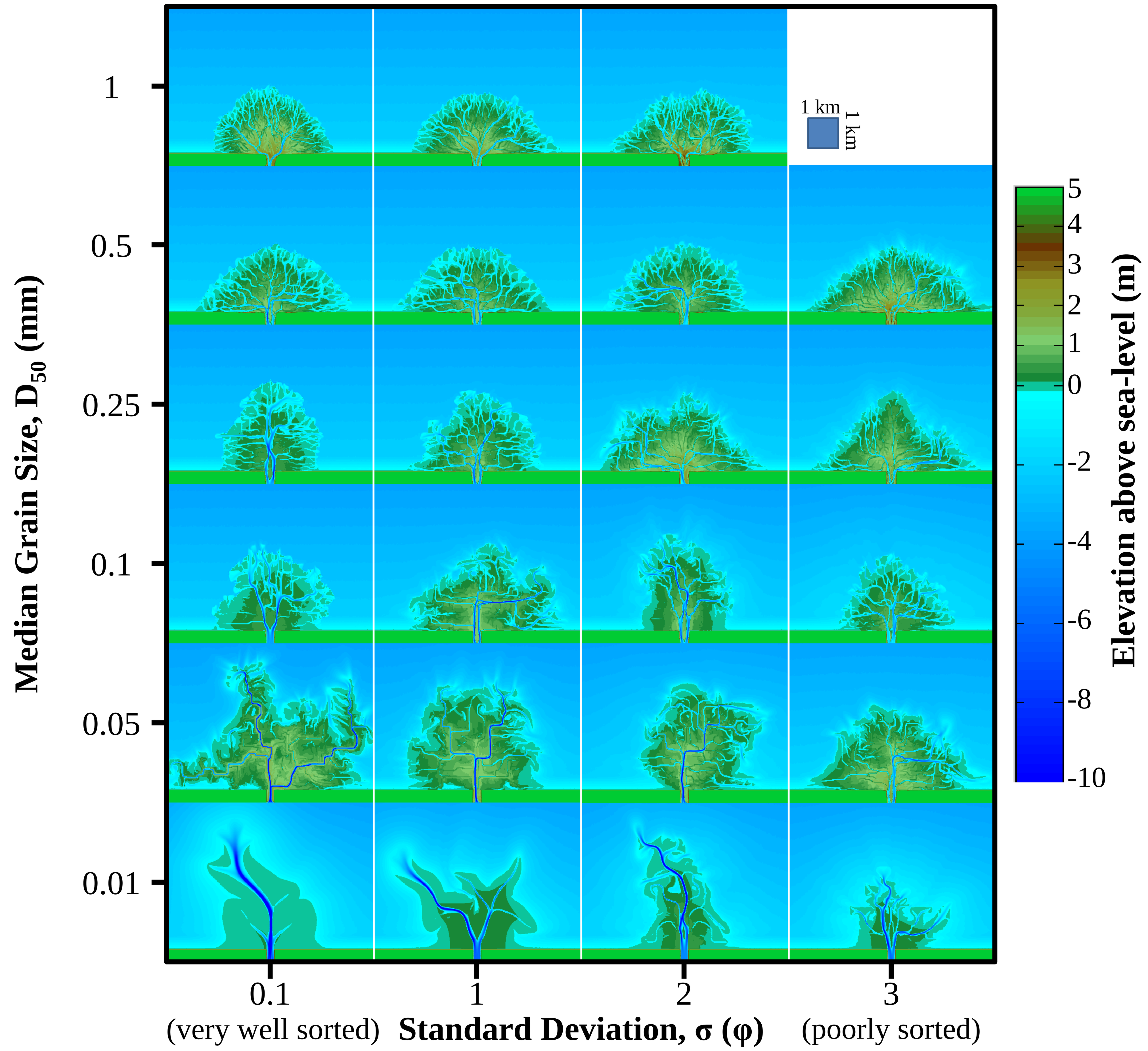

Figure 5. Delft3D model results that showing different delta morphologies created from changes to D_{50} and σ of the grain-size distribution. Images are taken when the same volume of sediment has entered the system.

Results suggest that changing the grain-size distribution creates the following trends:

- Low D_{50} and σ → low topset gradient, fewer channels, elongate shape
- High D_{50} and σ → steeper topset gradient, more channels, semi-circular shape
- Skewness results (not shown) have little effect on delta morphology

As D_{50} and σ increase a morphological transition occurs. To quantify this we measure the following morphometric parameters:

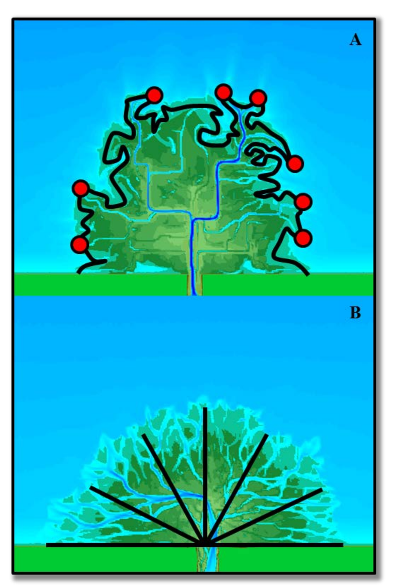

Number of Channel Mouths

1. Define active channel mouths by water depth, water velocity, and sediment flux thresholds
2. Average the number of channel mouths, present at a given time, throughout delta growth

Topset Gradient

1. Measure equally spaced rays from the delta head to points on the delta shoreline
2. Assume linear slopes and average rays for a representative gradient

Figure 6. (A) Black outline marks shoreline; red circles mark active channel mouths. (B) Topset gradient rays shown for every ~100 shoreline points. Example deltas correspond to grain-size distributions of D_{50} = 0.05 mm, σ = 1 φ (top panel), and D_{50} = 0.5 mm, σ = 2 φ (bottom panel).

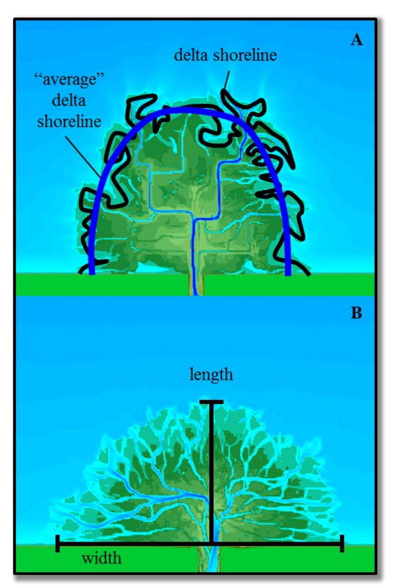

Shoreline Rugosity

1. Calculate as a sinuosity index:

$$\text{Rugosity} = \frac{\text{Delta Shoreline Length}}{\text{"Average" Shoreline Length}}$$

Bulk Delta Shape

1. Calculate a delta width to length ratio:

$$\text{Bulk Shape} = \frac{1}{2}\frac{\text{Delta Width}}{\text{Delta Length}}$$

Figure 7. (A) Black outline marks shoreline; blue line marks smoothed, or "average", shoreline (B) Lines mark delta length and width measurements. Example deltas from Fig. 6 are shown.

V. Analysis

Grain Size and Topset Gradient

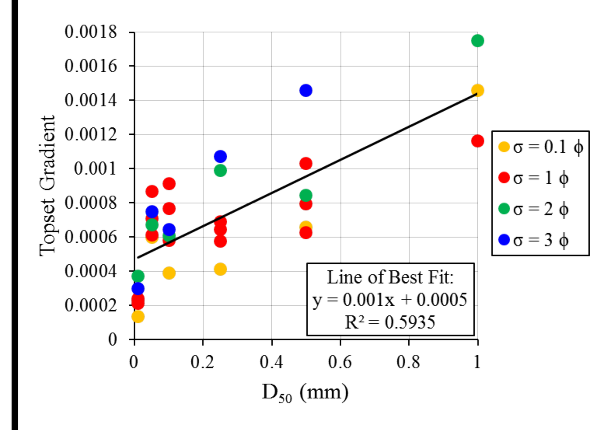

Figure 8. Relationship between D_{50} and topset gradient.

- Topset gradient increases linearly with respect to D_{50} (Fig. 8).
- Using normal flow equations, equilibrium topset gradients can be predicted as a function of sediment flux and median grain size (Fig. 9).

$$Gradient = K\sqrt{\frac{q_t}{q^2}D_{50}{}^{3/2}}$$

- The increase in topset gradient can be explained by an increase in D_{50} (R^2 = 0.62) using the equation above.

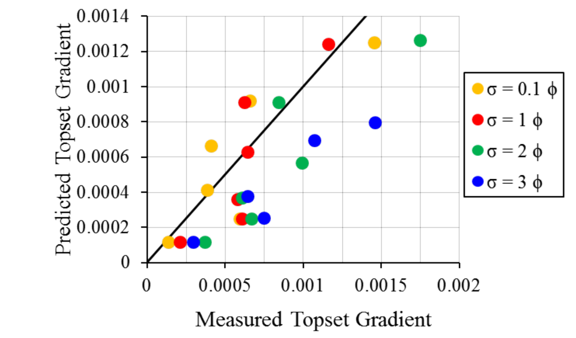

Figure 9. Plot of predicted topset gradients vs. measured topset gradients from model results. Black line denotes perfect agreement.

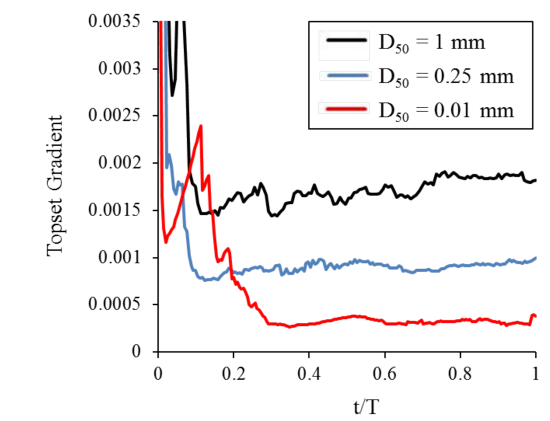

Figure 10. Topset gradient reaches a dynamic equilibrium after t/T ≈ 0.1, where t is time and T is total run time. Runs shown have σ = 2 φ

Grain Size and Number of Channel Mouths

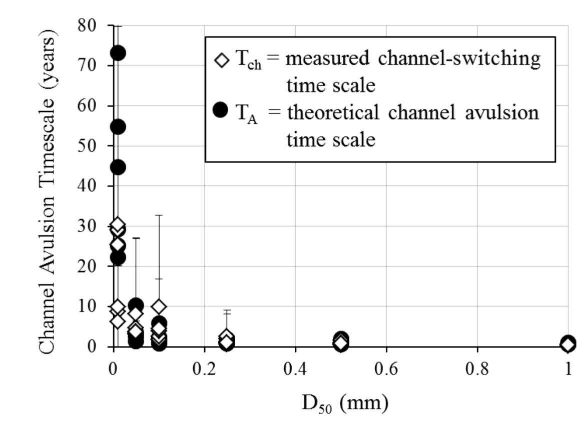

Figure 11. Measured T_{ch} and theoretical T_A values plotted against D_{50}. Vertical bars on T_{ch} represent measured standard deviation. T_A is calculated by the relation presented by Jerolmack and Mohrig, 2007, where T_A = average channel depth/channel aggradation rate.

- Topset gradient reaches a dynamic equilibrium (Fig. 10).
- To maintain steeper gradients, coarse-grained deltas aggrade faster, which leads to increased avulsion frequency and overbank flow (Fig. 11).
- Steeper gradients create overbank flows that exert higher shear stresses on the delta floodplain.
- Increased channel avulsion and overbank flow frequency creates a larger number of channels on coarse-grained deltas (Fig. 12).

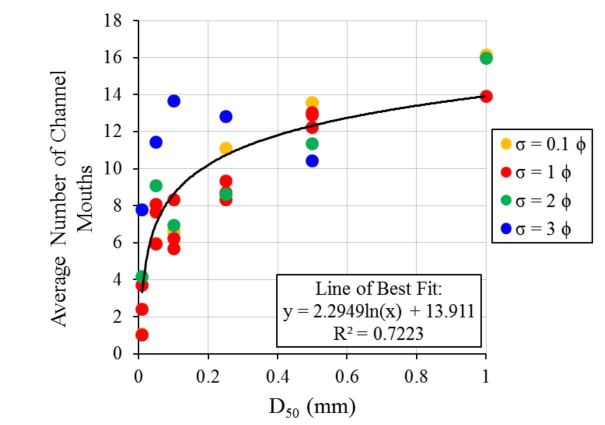

Figure 12. Relationship between D_{50} and average number of channel mouths.

VI. CONCLUSIONS

Process-based model for grain size effects on delta growth

Increase in Grain Size
↓ (+)
Topset Gradient (Fig. 8)
↓ (+)
Aggradation Rate (Fig. 10)
↓ (+)
Avulsion Frequency (Fig.11)
↓ (+)
Number of Channels (Fig. 12)
↓ (-)
Discharge per Channel Mouth
↓ (-)
Mouth Bar Growth
↓
Sets channel network and planform morphology (Fig. 5 and 13)

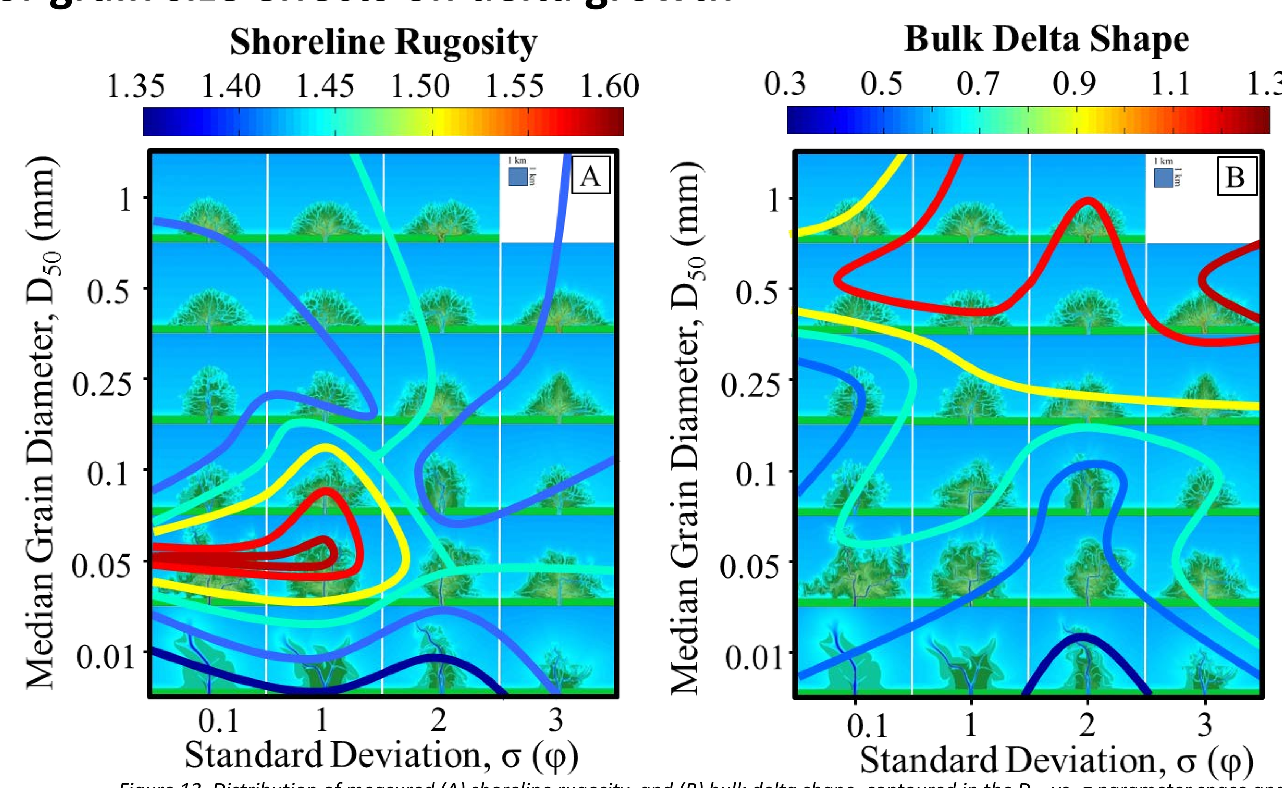

Figure 13. Distribution of measured (A) shoreline rugosity, and (B) bulk delta shape, contoured in the D_{50} vs. σ parameter space and superimposed on images of modeled deltas.

Coarse-grained deltas

- Bifurcations suppressed
- Sediment deposited evenly across shoreline
- Smooth shoreline, semi-circular shape (Fig. 13)

Medium-grained deltas

- Frequent bifurcations
- Local shoreline progradation
- Rugose shoreline, semi-circular shape (Fig. 13)

Fine-grained deltas

- Rare bifurcations
- Channel elongation by levee progradation
- Smooth shoreline, elongate shape (Fig. 13)

Jerolmack, D.J., and Mohrig, D., 2007, Conditions for branching in depositional rivers: Geology, v. 35, p. 463-466.

Orton, G.J., and Reading, H.G., 1993, Variability of deltaic processes in terms of sediment supply, with particular emphasis on grain size: Sedimentology, v. 40, p. 475-512.

Syvitski, J.P.M., and Saito, Y., 2007, Morphodynamics of deltas under the influence of humans: Global Planet Change, v. 57, p. 261-282.